

# INFLUENCE OF MICROSTRUCTURE ON MECHANICAL STRENGTH OF ALKALI-ACTIVATED Fe-Si-Ca RICH MATERIALS

Guilherme ASCENSÃO<sup>1,2,3</sup>, Flora FALESCHINI<sup>2</sup>, Maurizio MARCHI<sup>1</sup>, Monica SEGATA<sup>1</sup>, Yiannis PONTIKES<sup>3</sup>

<sup>1</sup> Italcementi S.p.A, HeidelbergCement group, 24126 Bergamo, Italy

<sup>2</sup> University of Padova, Department of Civil, Environmental and Architectural Engineering, 35131 Padova, Italy

<sup>3</sup> KU Leuven, Department of Materials Engineering, 3000, Leuven, Belgium

*ga.dossantos@italcementi.it, flora.faleschini@dicea.unipd.it, m.marchi@itcgr.net, m.segata@itcgr.net, yiannis.pontikes@kuleuven.be*

## Introduction

Enhanced Landfill Mining is a novel integrated waste management concept seeking the recovery of valuable resources from landfill sites. In the ELFM concept, the maximisation of valorisation of individual material streams is considered as critical for environmental sustainability and economic viability of the concept. The gasification and vitrification of refuse derived fuel (RDF) derived from ELFM is expected to generate significant volumes of Fe-Si-Ca rich residues<sup>1,2</sup> of which the use as inorganic polymers (IP) precursors has been identified as a promising valorisation route.<sup>3,4</sup>

The use of these residues, commonly termed plasmastone as an IP precursor is incipient<sup>5</sup> and suggested applications include – among others - pavers<sup>3</sup>, mortars<sup>4</sup> and insulating building materials.<sup>6</sup> Aiming to contribute to the design and conceptual development of novel value-added plasmastone-based products, the present work aspires to identify the effect of different processing parameters on the synthesis of such IP binders. A Design of Experiments (DoE) methodology was used to evaluate the effect of three main compositional factors, their interaction, and the system responses.

## Experimental

A “Two-Level-Full-Factorial” design with a central point was employed in order to assess the influence of three variables (solid-to-liquid ratio,  $K_2O/SiO_2$  molar oxide ratio of mixture (solids and activating solution) and the KOH solution molarity) on IP properties. Their minimum and maximum values and the description of the experimental design are given in Table 1. A synthetic glass (further termed as PS) was used as IP precursor and its detailed production process can be found elsewhere.<sup>3</sup>

The glass was dried, homogenised and milled to a Blaine surface of approximately 360 m<sup>2</sup>/kg; and is composed of (in wt%) SiO<sub>2</sub> 35.1, CaO 22.9, Fe<sub>2</sub>O<sub>3</sub> 22.8, Al<sub>2</sub>O<sub>3</sub> 16.1, MgO 1.4, K<sub>2</sub>O 0.6, TiO<sub>2</sub> 0.6, Na<sub>2</sub>O 0.3, Mn<sub>2</sub>O<sub>3</sub> 0.1, SO<sub>3</sub> 0.1 and 1.9% loss on ignition (LOI). Commercially available Si and Si-Al rich powdered material were used as admixtures, at levels not exceeding 10 wt%. The use of M-silicates, where M is Na and/or K, was avoided to reduce IPs production cost.<sup>7</sup> Potassium hydroxide solutions were used to provide the alkaline medium and demineralised water was added to achieve the pre-defined S/L ratio. In PS3 and PS8 samples additional 7.69 g/kg<sub>slurry</sub> of demineralised water was provided to achieve the required flowability to allow proper casting of the samples. The mixture followed the procedure described elsewhere,<sup>8</sup> but mixing speed was increased to 140 rpm. The slurries were cast into 4x4x16 cm<sup>3</sup> moulds and cured for 24 h at 20 °C and 95% RH. Afterwards, the samples were demoulded and kept at room conditions (20 °C and 65% RH).

X-ray fluorescence was used to determine the chemical composition of the raw materials. The IPs' mineralogical composition was assessed by X-ray diffraction. Scanning electron microscopy equipped with energy dispersive X-ray spectrometry was used to evaluate IPs microstructure. Archimedes method was employed to evaluate the IP water absorption. Open porosity was estimated as described in literature<sup>8</sup> while IPs' apparent density was determined by the relation between the weight and volume of each sample. The flexural and compressive strength of the cured IP samples were determined according to the EN196-1:2016. The experimental error was assessed by testing two samples for each formulation and curing age that were produced independently one from the other.

**Table 1:** DoE experimental plan

| Code                              | PS1   | PS2   | PS3   | PS4   | PS5   | PS6   | PS7   | PS8   | PS9   |
|-----------------------------------|-------|-------|-------|-------|-------|-------|-------|-------|-------|
| S/L                               | 2.50  |       | 2.90  |       | 2.70  | 2.50  |       | 2.90  |       |
| K <sub>2</sub> O/SiO <sub>2</sub> | 0.200 | 0.170 | 0.200 | 0.170 | 0.185 | 0.200 | 0.170 | 0.200 | 0.170 |
| KOH mol/L                         | 14    |       |       |       | 12    | 10    |       |       |       |

## Results and discussion

Figure 1a and 1b show representative SEM micrographs of samples after 28 days of curing. Unreacted particles showed that precursors' complete dissolution did not occur. The high content of solid precursors limited dissolution, but all samples exhibited a homogeneous matrix where undissolved particles act as small-sized aggregates. The K<sub>2</sub>O/SiO<sub>2</sub> molar oxide ratio seemed to affect the degree of dissolution while the change in KOH molarity induced less pronounced microstructural changes. Comparing samples with similar S/L and KOH molarity, *e.g.* PS1 and PS2 (Figure 1), suggests that as the K<sub>2</sub>O/SiO<sub>2</sub> molar oxide ratio decreases, the content of unreacted

particles rises. Still, quantitative analysis is needed to describe the impact of the investigated compositional factors on precursors' degree of dissolution. EDS analyses revealed a binder phase predominantly composed of Si, Al, Fe, Ca and K, while undissolved particle spectra were in line with PS chemical composition. Elemental mapping did not suggest crystalline precipitations, in line with XRD data and SEM observations. The XRD patterns of the IP revealed their amorphous nature, with only one low-intensity crystalline diffraction peak identified as calcite (diffraction patterns not shown here for sake of brevity).

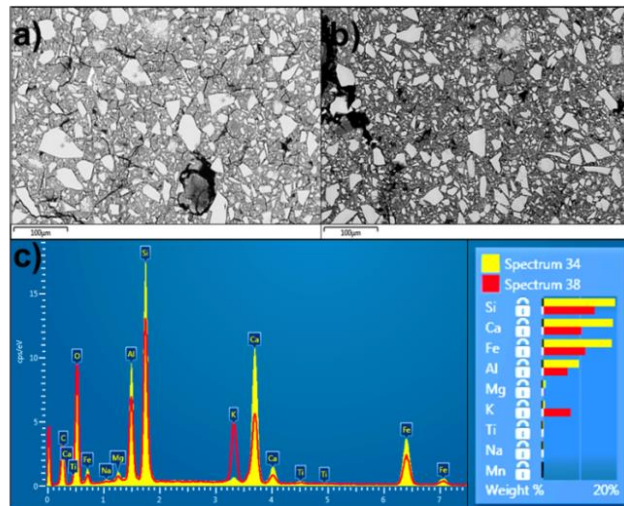


**Figure 1:** SEM micrographs of sample PS1 (a) and PS2 (b) and representative EDS spectra from sample PS1 where spectrum #34 shows PS unreactive particles and spectrum #38 the binder (c).

Spherical large size pores were observed and can be attributed to entrapped air during mixing; no correlation was found between their amount and size and the studied compositional parameters. Length and size of micro-cracks seem to be governed by the  $K_2O/SiO_2$  molar ratio. Three simultaneous effects may contribute to such behaviour: (i) crack development and propagation being limited by the presence of undissolved particles which was incremented by lowering the  $K_2O/SiO_2$  molar ratio<sup>4</sup>; (ii) a delay effect on elasticity development, as higher  $H_2O/K_2O$  ratios<sup>9</sup> decrease the rate of IP binder formation, resulting in lower autogenous shrinkage and (iii) lower polymerisation degree resulting in less intensive exothermic reaction, hence decreasing the internal temperature during the polycondensation process.<sup>3</sup> Nonetheless, such pores and micro-cracks did not have a significant influence on the overall open porosity and water absorption capacity of the IPs, suggesting their closed nature and low connectivity. Still,  $S/L$  seems to determine density and open porosity, whereas increasing the  $K_2O/SiO_2$  ratio contributes to further densification. Rising the  $K_2O/SiO_2$  ratio maximises the binder formation, leading to a more homogenous binder matrix. Regardless of the beneficial effect of limiting crack formation, samples PS3 and PS8 showed the lowest water absorption and open

porosity values. The KOH molarity impact can also be seen, and samples produced with 10 M KOH solution are slightly less porous than their 14 M KOH counterparts. In fact, by combining high *S/L* and  $K_2O/SiO_2$  ratios and using 10 M KOH solution the highest density was achieved ( $2.30 \pm 0.02 \text{ g/cm}^3$ ).

**Table 2:** IPs apparent density, open porosity, water absorption, flexural and compressive strength and corresponding standard deviations after 28 days of curing

| Code | Apparent density ( $\text{g/cm}^3$ ) | Open porosity (%) | Water absorption (%) | Flexural strength (MPa) | Compressive strength (MPa) |
|------|--------------------------------------|-------------------|----------------------|-------------------------|----------------------------|
| PS1  | $2.21 \pm 0.00$                      | $2.27 \pm 0.07$   | $1.04 \pm 0.03$      | $2.8 \pm 0.0$           | $88.2 \pm 0.4$             |
| PS2  | $2.13 \pm 0.01$                      | $2.99 \pm 0.16$   | $1.41 \pm 0.07$      | $2.2 \pm 0.3$           | $76.1 \pm 1.5$             |
| PS3  | $2.29 \pm 0.04$                      | $0.93 \pm 0.01$   | $0.41 \pm 0.01$      | $5.1 \pm 0.2$           | $94.2 \pm 0.0$             |
| PS4  | $2.27 \pm 0.01$                      | $1.50 \pm 0.02$   | $0.67 \pm 0.01$      | $3.3 \pm 0.9$           | $93.8 \pm 6.2$             |
| PS5  | $2.21 \pm 0.01$                      | $1.34 \pm 0.18$   | $0.61 \pm 0.08$      | $3.3 \pm 0.1$           | $94.6 \pm 2.4$             |
| PS6  | $2.20 \pm 0.01$                      | $1.55 \pm 0.39$   | $0.71 \pm 0.18$      | $3.0 \pm 0.3$           | $78.9 \pm 3.4$             |
| PS7  | $2.13 \pm 0.01$                      | $2.10 \pm 0.07$   | $0.99 \pm 0.04$      | $2.5 \pm 0.7$           | $75.0 \pm 1.6$             |
| PS8  | $2.30 \pm 0.02$                      | $0.68 \pm 0.18$   | $0.29 \pm 0.09$      | $6.0 \pm 1.5$           | $93.6 \pm 0.1$             |
| PS9  | $2.25 \pm 0.01$                      | $1.16 \pm 0.09$   | $0.52 \pm 0.04$      | $4.2 \pm 0.1$           | $105.5 \pm 5.2$            |

IPs mechanical properties were measured after 7 and 28 days of curing and the highest mechanical performances were achieved with samples produced with *S/L* = 2.90, namely samples PS3, 4, 8 and 9 (Table 2). Flexural strength diminishes over time, while the compressive strength exhibits the opposite trend (only 28<sup>th</sup> day data shown here for sake of brevity). As previously reported,<sup>8</sup> the polymerisation reactions are not concluded after 7 days of curing and the on-going reorganisation of the structure leads to an increase of compressive strength over time. Nonetheless, the increase of rigidity of highly cross-linked structures can lead to poor flexural performances. In fact, a reduction of IP flexural strength over time was observed in all samples (ranging from 14.8 to 46.0%). The different relative influence of each compositional parameter and their synergetic effects on strength development can be depicted through its standardised effect, shown in Figure 2, while the flexural and compressive responses are shown in Figure 3.

In general, decreasing the *S/L* ratio is detrimental to strength development and its dominant character affects both flexural and compressive strength. KOH molarity assumes a significant role regarding the flexural strength development while its synergistic effects with *S/L* and  $K_2O/SiO_2$  has a significant impact on compressive strength (Figure 2). In high *S/L* formulations, rising  $K_2O/SiO_2$  molar ratio promoted better flexural strengths, whereas in samples prepared with lower *S/L* ratio no significant changes occurred. Compressive strength was particularly enhanced when

$K_2O/SiO_2$  ratio was raised in formulations prepared with  $S/L = 2.50$ , but no evident beneficial effect can be seen in higher  $S/L$  ratios (Figure 3).

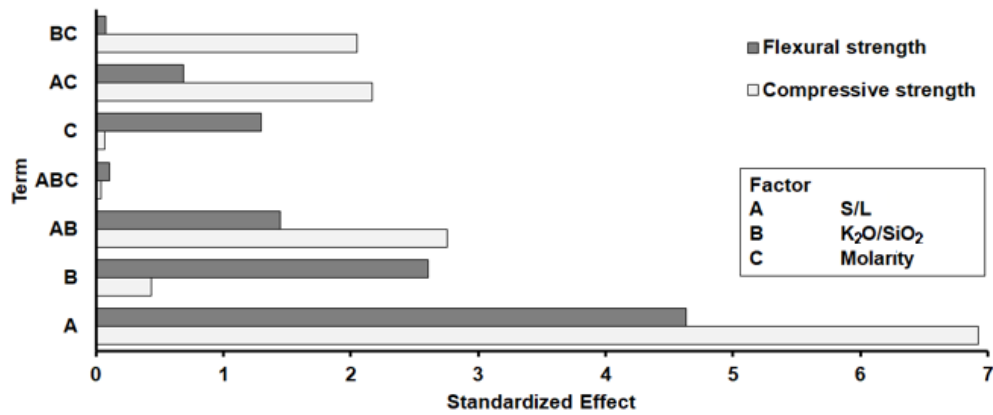


**Figure 2:** Standardised effect of compositional parameters on flexural and compressive strength after 28 days of curing

In IP synthesis, compositional and processing parameters are often considered individually underestimating their combined effects. The results presented herein confirmed the relevancy of synergic effects on IPs properties (as identifiable in Figure 2) and corroborate the necessity for more elaborative models, integrating not only singular compositional parameters but also their combined effects. These subjects will be addressed by the authors in future works.

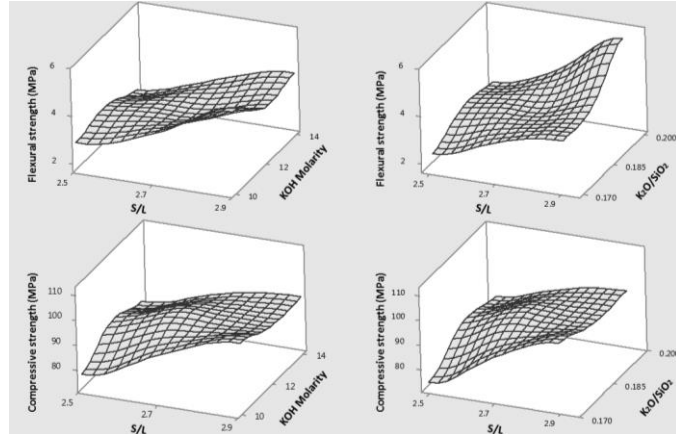


**Figure 3:** Influence of compositional parameters and their synergetic effects on IPs flexural and compressive strength after 28 days of curing

## Conclusions

In the present work, Fe-Si-Ca rich inorganic polymeric binders (IPs) were synthesised with high contents of Fe-Si-Ca rich residues (86.7 wt%), no Na,K-silicate solutions and low curing temperature (20°C). Results showed that IP properties can be controlled by proper mix design. Solid-to-liquid and  $K_2O/SiO_2$  ratios were found to be the main

governing factors, whereas the influence of KOH molarity was less significant for the investigated IP properties. The produced IPs presented low open porosity (< 3.0%) and water absorption (< 1.41%), and considerable flexural (up to 6 MPa) and compressive strength (up to 105.5 MPa) after 28 days of curing. Further research should be conducted to assess the influence of other compositional (*e.g.* SiO<sub>2</sub>/Al<sub>2</sub>O<sub>3</sub>, SiO<sub>2</sub>/(Al<sub>2</sub>O<sub>3</sub>+Fe<sub>2</sub>O<sub>3</sub>)) and processing factors (*e.g.* mixing, curing conditions). The results herein constitute the first contribution towards a model where Fe-Si-Ca-rich IP binder properties can be predicted and tailored by adjusting the mix design while suppressing the production cost. This approach will ultimately make these materials more attractive for real-life applications, and by doing so, facilitates the transition to a circular economy.

## Acknowledgements

This project has received funding from the European Union's Horizon 2020 research and innovation programme under the Marie Skłodowska-Curie grant agreement No 721185 (EU MSCA-ETN NEW-MINE).

## References

1. M. Danthurebandara, S. Van Passel, L. Machiels, and K. Van Acker, "Valorization of thermal treatment residues in enhanced landfill mining: environmental and economic evaluation", *J Clean Prod*, **99** 275-285 (2015).
2. A. Bosmans, I. Vanderreydt, D. Geysen, and L. Helsen, "The crucial role of Waste-to-Energy technologies in enhanced landfill mining: a technology review", *J Clean Prod*, **55** 10-23 (2013).
3. L. Machiels, L. Arnout, P. Yan, P. T. Jones, B. Blanpain, and Y. Pontikes, "Transforming Enhanced Landfill Mining Derived Gasification/Vitrification Glass into Low-Carbon Inorganic Polymer Binders and Building Products", *J Sust Metall*, **3** (2) 1-11 (2017).
4. L. Machiels, L. Arnout, P. T. Jones, B. Blanpain, and Y. Pontikes, "Inorganic polymer cement from Fe-silicate glasses: varying the activating solution to glass ratio", *Waste Biomass Valori*, **5** 411-428 (2014).
5. Marie Skłodowska-Curie Actions, Innovative Training Networks, H2020-MSCA-ITN-2016- NEW-MINE-Grant Agreement No 721185.
6. L. Kriskova and Y. Pontikes, "Effect of activating solution on the synthesis and properties of porous Fe-Si-Ca rich inorganic polymers", in *Proceedings of the 5<sup>th</sup> International Slag Valorisation Symposium* (pp. 449-452), edited by R. Iacobescu and A. Malfliet, Leuven, Belgium, 2017.
7. G. Ascensão, M. P. Seabra, J. B. Aguiar and J. A. Labrincha, "Red mud-based geopolymers with tailored alkali diffusion properties and pH buffering ability", *J Clean Prod*, **148** 23-30 (2017).
8. L. Arnout, L. Kriskova, S. Onisei, L. Machiels, B. Blanpain and Y. Pontikes, "Effect of the activating solution's chemistry and volume, on the processing and properties of Fe-Si-Ca-rich inorganic Polymers", in *Proceedings of the 5<sup>th</sup> International Slag Valorisation Symposium* (pp. 341-344), edited by R. Iacobescu and A. Malfliet, Leuven, Belgium, 2017.
9. G. Beersaerts, L. Arnout, L. Machiels, J. Elsen and Y. Pontikes, "Monitoring early-age crack formation in Ca-Fe-Al-rich inorganic polymers", in *Proceedings of the 5<sup>th</sup> International Slag Valorisation Symposium* (pp. 345-348), edited by R. Iacobescu and A. Malfliet, Leuven, Belgium, 2017.